Contents list available at IJRED website

International Journal of Renewable Energy Development

Journal homepage: https://ijred.undip.ac.id

Research Article

Experimental thermal and electrical performances of a PVT-air collector coupled to a humidification-dehumidification (HDH) cycle

Ahmed Ghazy*

Mechanical Engineering Department, College of Engineering, Jouf University, Sakaka, Al-Jouf, Saudi Arabia

Abstract. Despite their low electrical efficiencies, PVs are widely used to generate electricity from abundant solar energy. In order to maximize the utilization of incident solar energy, PVT collectors have been used to simultaneously generate electricity and thermal energy. Furthermore, combining PVTs with humidification-dehumidification (HDH) cycles can provide electricity and potable water in remote, arid rural areas that are not connected to the grid. In this paper, a PVT-air collector was coupled to an air-heated closed HDH cycle. Air was heated within the PVT collector and humidified by saline water spray inside the humidifier. Fresh water was produced by cooling humid air inside a dehumidifier that is cooled by saline water. The thermal and electrical performances of the PVT-HDH system were experimentally studied and compared to the electrical performance of a PV module with similar characteristics. The results demonstrated a significant decrease in PV temperature within the PVT-HDH system, which resulted in a 20% increase in the output power of the PVT-HDH system at midday compared to the identical PV module. In addition, the PVT-HDH system produced about 3.8 liters of water distillate for a PV module surface area of 1.48 m × 0.68 m, which contributed about 38% to the overall efficiency of the PVT-HDH system.

Keywords: PVT-air Collector, Thermal Efficiency, Electrical Efficiency, Humidification-Dehumidification

Received: 15th January 2023; Revised: 20th March 2023; Accepted: 4th April 2023; Available online: 11th April 2023

1. Introduction

The rapid and continuous increase in global energy demand as a result of industrial and economic growth has resulted in a massive increase in the consumption of fossil fuels. Carbon emissions from fossil fuel combustion are considered the primary cause of severe ecosystem problems such as climate change and global warming. Due to the severe degradation of our ecosystem and the near depletion of fossil fuels, there is an urgent need to investigate eco-friendly energy sources. Meanwhile, it is believed that switching to renewable energy sources such as solar and wind energies will simultaneously solve the energy crisis and save the environment.

Solar energy, in particular, is abundant and can be harvested in both thermal and photovoltaic forms using solar collectors and photovoltaic cells, respectively. However, the usefulness of solar energy is still quite low. For example, the electrical efficiency of photovoltaic (PV) modules, which have been widely used to convert solar energy to electricity, does not exceed 20% (Browne *et al.,* 2016). This is because the majority of incident solar energy is either reflected into the environment or absorbed by the PV module and converted into unwanted heat, which in turn reduces the electrical efficiency of the PV module by about 0.5% for every 1oC increase in temperature (Brahim *et al.,* 2017). In addition, the thermal stresses generated in the PV modules due to a prolonged rise in their temperatures may damage their structures. Therefore, extensive research work has been conducted on various active and passive cooling techniques for PV modules. For instance, Bayrak *et al.* (2019) investigated the influence of different fin configurations placed on the back of a PV module on its cooling by natural air convection. Rezvanpour *et al.* (2020) reduced the temperature of the PV module by 38% and increased its output power by 24.68% in cold weather by using phase change material. Mehrotra *et al.* (2014) found that immersing the PV module in 1 cm of water increased its efficiency by 17.8 %. Alami (2014) increased the output power of a PV module by 19.1% by utilizing passive evaporative cooling on the back of the PV module. Nizetic *et al.* (2016) improved the efficiency of the PV module by 14.4% by sprinkling water on its surface.

In addition, combining PVs with solar collectors in Photovoltaic/Thermal (PVT) and concentrated Photovoltaic/Thermal (CPVT) systems to simultaneously produce electricity and heat from the same incident solar irradiation can significantly improve the overall system efficiency at a small additional cost. The heat produced can be used for a variety of purposes, including water heating (Abdul-Ganiy *et al.,* 2021), space cooling and heating (Herrando *et al.,* 2019), crop drying (Fterich *et al.,* 2018), and desalination of saltwater (Calise *et al.,* 2019). Nevertheless, the solar collectors used in these applications range from concentrating collectors, such as Parabolic Trough Collectors (PTC) (Widyolar *et al.,* 2017), Parabolic Dish Collectors (PDC) (Singh *et al.,* 2020), and Linear Fresnel Reflectors (LFR) (Pham *et al.,* 2018), to non-

* Corresponding author
Email: aeghazy@ju.edu.sa (A.Ghazy)

https://doi.org/10.14710/ijred.2023.51808
ISSN: 2252-4940/© 2023.The Author(s). Published by CBIORE

concentrating collector such as Flat Plate Collectors (FPC) (Moss *et al.,* 2018) based on the output temperature range.

Recently, there has been increased interest in desalination systems powered by heat generated by PVTs and CPVTs. In this context, Tiwari *et al.* (2020) used a photovoltaic thermal-compound parabolic concentrator (PVT-CPC) to supply a single basin solar still with hot water. Naroei *et al.* (2018) increased the water production of stepped solar still by 20% by connecting a PVT-water collector to the still. Singh (2018) studied the effect of attaching N identical PVT-CPCs and PVT-CPCs to conventional solar stills (CSS) on the improvement of their performances. The study revealed that the use of PVT-FPCs reduced the cost of water production by 2.3% and 27.05% compared to CSS and PVT-CPC, respectively. Monjezi et al. (2020) concluded that preheating seawater in a PVT-water collector prior to introducing it to a reverse osmosis (RO) unit can reduce the electricity consumption rate of RO desalination by 0.12 kWh/m^3.

Furthermore, solar desalination using the humidification-dehumidification (HDH) technique (Fath *et al.,* 2002 and Narayan *et al.,* 2010) is one of the thermal desalination methods with a simple structure and low operating temperature (He *et al.*, 2016a and 2016b), which made it much easier to be coupled with solar collectors (Bacha, 2013 and Ghazy *et al.,* 2016). Solar HDH can be classified as air-heated HDH and water-heated HDH depending on the fluid being heated by solar energy. For example, saline water can be heated by a flat plate solar collector (Zeman *et al.,* 2009; Soufari *et al.,* 2009a and Soufari *et al.*, 2009b), by an evacuated tube water collector (Hamed *et al.,* 2015), or by a PV-driven heater (Wang *et. al.,* 2012). On the other hand, air can also be heated by an evacuated tube solar heater (Antar & Sharqawy, 2013), by an all-glass evacuated tubes solar air heater (Li *et al.*, 2014), or by the condensation losses of a solar still (Ghazy & Alrowais, 2022). In addition, Zhani *et al.* (2011) and Deniz & Cinar (2016) studied the heating of both air and water in HDH and Yildirim & Solmus (2014) studied the operation of HDH on air, water, and hybrid air and water heating modes.

Coupling HDH with PVTs enabled the utilization of the produced thermal energy from the PV module to drive the HDH cycle and produce potable water (Anand & Srinivas, 2017). In this context, Gabrielli *et al.* (2019) numerically investigated the optimal design and operation conditions of an HDH cycle coupled to PVT-water. The study concluded that maximum water production was attained when operating at the maximum possible saline water flow rate, which was achieved by the use of two PV modules connected in series. Elsafi (2017) modeled a CPVT combined with an air-heated HDH cycle. The model predicted an annual freshwater and electricity production of 12 m^3 and 960 kWh, respectively for annual solar irradiance of 1.88 MWh. However, despite the simplicity and affordability of air heating for the HDH cycle, air cannot effectively cool the elevated temperature of the CPV. In addition, the electrical and thermal performances of the PVT were evaluated independently and approximately by these models. Pourafshar et al. (2020) introduced a double-pass PVT collector as a humidifier for an HDH cycle with a heat pump. The experimental results showed a freshwater production rate of 0.56 to 0.99 kg/h per unit area of the PV module, however, the presence of a glass cover above the PV module decreases the solar irradiance it received and, consequently, its electricity generation.

The literature review reveals that previous studies on coupling PVs with HDH lacked a balance between the electrical efficiency of the PV module and the thermal efficiency of the PV-HDH system as a whole. The majority of the studies compromised the electrical efficiency of the PV module in favor of enhancing the fresh water yield of the HDH cycle. However, coupling PVs with HDH should first consider improving the electrical efficiency of the PV module as the primary system, followed by enhancing the PV-based HDH cycle as the secondary system. In addition, more consideration should have been given to the cost and simplicity of the HDH cycle. Accordingly, it can be concluded that air-heated HDH cycles are advantageous to water-heated ones in terms of both cost and simplicity, especially when natural air circulation is taken into account. In addition, PVTs are preferable to CPVTs due to the huge temperature rise of CPVTs, which dramatically degrades the electrical efficiency of the PV module unless extremely effective cooling strategies are employed. Moreover, glass-covered PVTs are unfavorable because of the reduction in the solar energy received by the PV module and the module's thermal losses to the surrounding air. Consequently, this study aims to experimentally investigate the thermal performance of a simple PVT-air collector coupled to a closed air-heated HDH cycle. In addition, the enhancement in the electrical efficiency of the PVT was assessed and compared to that of a PV module with identical characteristics.

2. Experimental Set Up

This section describes the technical specifications and operating parameters of the PVT-HDH system. Following that, the experimental methodology and performance parameters used to evaluate the performance of the PVT-HDH system are discussed.

2.1 System Description

Fig 1(a) shows a schematic diagram of the PVT-HDH system, while Fig 1(b) shows the actual setup. The PVT-HDH systems consisted of a PVT-air collector, a humidifier, a dehumidifier,

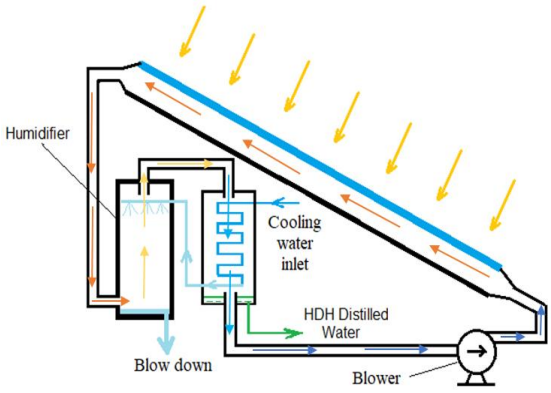

(a)

(b)

Fig 1. PVT-HDH (a) scheme and (b)experimental setup.

Table 1
PV module characteristics.

Parameters	Values
Peak power	150 W
Open-circuit Voltage	21.6 V
Maximum power current	8.78 A
Maximum power voltage	12 V
Short-circuit current	9.58 A
Cell technology	Monocrystalline Silicon
Module dimensions	1.48 ×0.68 m

and an air blower that circulated air through these components in a closed loop. The PVT-air collector consisted of a blackened galvanized steel duct sized 1.48 ×0.68×0.1 m with a 3 mm sheet thickness. The PV module comprised the top of the air duct, which was inclined 30° against the horizontal plane to maximize solar collection. The humidifier was a plastic drum through which air entered from a lower side hole and exited from an upper side hole, saline water was sprayed from nozzles on the top, and concentrated brine blow down exited from the bottom. The dehumidifier was a plastic drum through which air entered from an upper side hole and exited from a lower side hole, saline cooling water entered a copper coil, inside the dehumidifier, from an upper side hole and exited from a lower side hole, and fresh water was collected from the bottom. In order to recover the condensation energy of the dehumidifier, heated brine water from the dehumidifier was sprayed over the airflow inside the humidifier. In addition, the bottom and sides of the PVT-air collector were insulated with a 5 cm thick extruded polystyrene board, and the humidifier, dehumidifier, and connecting ducts were insulated by a flexible insulation sheet to minimize thermal losses from the PVT-HDH system.

2.2 Experimental methodology

The PVT-HDH was experimentally tested side-by-side against a PV module with identical characteristics under the climate conditions of Sakaka (29.9° N, 39.3° E), Saudi Arabia. The characteristics of the PV modules are detailed in Table 1. Temperatures were measured using K-type thermocouples, the solar intensity was measured using a digital pyranometer, airflow and ambient wind velocities were measured using a digital anemometer, PV characteristics were measured using a PV analyzer, and water distillate was measured using a measuring jar. Table 2 lists the measuring ranges, accuracies, and errors of the measuring devices used to obtain experimental data.

The measured parameters were utilized in evaluating the thermal and electrical performances of the PVT-HDH system and the identical PV module.

2.3 Performance analysis

The electrical efficiencies (η_{ele}) of the PV module in the PVT-HDH system and the conventional PV module were calculated by Eq 1.

$$\eta_{ele} = \frac{\sum P_{max}}{\sum I(t) \times A} \quad (1)$$

where P_{max} (W) is the maximum output power of the PV module, $I(t)$ (W/m^2) is the incident solar irradiation on the PV module, and A (m^2) is the PV module area.

The thermal efficiency (η_{th}) of the PVT-HDH system was calculated by

$$\eta_{th} = \frac{\sum(M_{HDH} \times h_{fg}(T))}{\sum I(t) \times A} \quad (2)$$

where M_{HDH} (kg) is water distillate from the HDH cycle, $h_{fg}(T)$ (J/kg) is the temperature-dependent latent heat of saline water vaporization.
The overall efficiency (η_{ov}) of the PVT-HDH was calculated by summing its thermal and electrical efficiencies as follows.

$$\eta_{ov} = \eta_{ele} + \eta_{th} = \frac{\sum P_{max} + \sum(M_{HDH} \times h_{fg}(T))}{\sum I(t) \times A} \quad (3)$$

3. Results and Discussion

The weather conditions measured in Sakaka (29.9° N, 39.3° E), Saudi Arabia in August is shown in Fig 2. The measured solar intensity increased steadily from the mooring to about 1200 W/m^2 at midday, and then gradually decreased until sunset. The measured ambient temperature increased from about 30 °C at 7.00 a.m. to about 45°C at 1.00 p.m., then decreased to about 37°C at sunset. The surrounding wind velocity varied throughout the day from 1 m/s to 3 m/s.

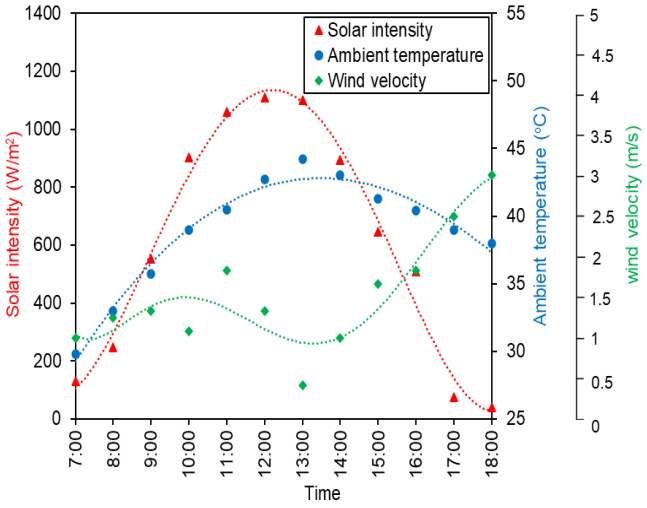

Fig 2. Climate conditions at Sakaka, Saudi Arabia in August.

Table 2
Measuring devices features.

Measured variable	Measuring device	Measuring range	Measuring accuracy	Measuring error
Temperatures	K-type thermocouples	-50 to 400°C	±1°C	2%
Solar irradiation intensity	digital pyranometer	0 to 3999 W/m^2	±10 W/m^2	3%
Airflow speed	digital anemometer	0.1 to 30 m/s	±0.1 m/s	1%
Water distillate	measuring jar	1000 mL	10 mL	
PV characteristics	PV analyzer	10 to 60 V	0.01 V	1%
		0.01 to 10 A	1 mA	1%

3.1 Thermal performance

Fig 3(a) compares the hourly surface temperature of the PV module in the PVT-HDH system to that of a conventional PV module. Compared to the ambient air temperature, the temperatures of both modules steadily increased from mooring until early afternoon and then decreased until sunset. Moreover, the temperature of the PV module in the PVT-HDH system was consistently lower than that of the conventional PV module. In addition, the maximum temperature of the conventional PV module was about 10°C higher than that of the PV module in the PVT-HDH system and about 20°C higher than the ambient temperature. These findings are consistent with the results of Jaszczur *et al.* (2021).

The temperature distribution within the PVT of the PVT-HDH system is illustrated in Fig 3(b). The air temperatures within the PVT collector are observed to follow the same pattern as the ambient air temperature, despite being consistently higher than the ambient air temperature throughout the day. Moreover, the air temperature difference between the inlet and the outlet of the PVT collector increased steadily throughout the day until midday, when the temperature difference reached 10°C, and then decreased until sunset. These results agree well with the measured data by Joshi *et al.* (2009).

Fig 4(a) depicts the hourly variation in the temperatures of the circulating air and sprayed saline water within the humidifier of the PVT-HDH. Despite the constant increase in the temperature of the sprayed saline water inside the humidifier, the air temperature difference between the humidifier's exit and inlet increased steadily until midday, when a temperature difference of about 15°C was reached. This is due to the noticeable rise in humidifier inlet air temperature during the day. However, the cooling of the air inside the humidifier gradually diminished from midday until sunset.

The temperature distribution of the circulating air and saline cooling water inside the dehumidifier is shown in Fig 4(b). Observations indicate that the difference in air temperature between the dehumidifier's inlet and outlet grew until midday and then decreased afterward. In addition, the cooling of the air mandated the heating of the saline cooling water. For instance, during midday, airt was cooled by about 6°C while saline cooling water was heated by about 4°C. The temperatures distributions within the humidifier and the dehumidifier are in agreement with the experimental data obtained by Ghazy& Alrowais (2022).

The hourly variation in the psychometric properties of the air during the cooling and humidification process inside the humidifier is illustrated in Fig 5(a). Air humidification is represented by an increase in the air's specific humidity (y-axis), while air cooling is represented by a decrease in the dry bulb temperature (x-axis). It is noticeable that both the dry bulb temperature and specific humidity of the air steadily increased until midday and then decreased until sunset.

Fig 5(b) illustrates the cooling and dehumidification process of air inside the dehumidifier. Air dehumidification is represented by a reduction in the specific humidity of the air,

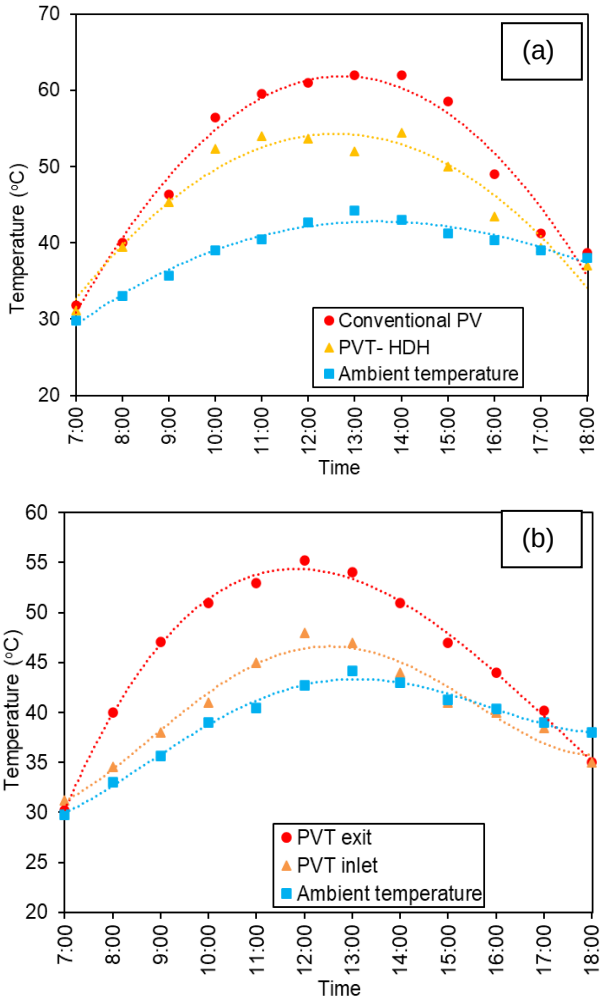

Fig 3. (a) PV and (b) air temperatures within the PVT-air collector.

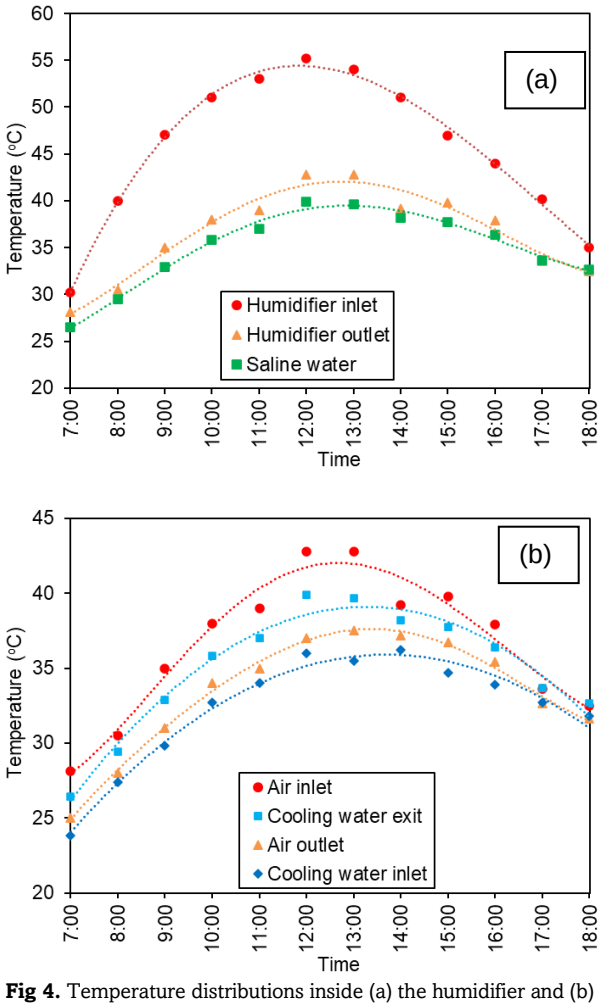

Fig 4. Temperature distributions inside (a) the humidifier and (b) the dehumidifier of the PVT-HDH system.

Table 3
Comparison between distillate production of the present study and previous PVT-HDH systems.

HDH system	Distillate production (L/h. m^2)	Reference
PVT-HDH with heat pump	0.99	Pourafshar *et al.* (2020)
PVT-water coupled with HDH system	0.82	Anand & Srinivas (2017)
PVT-air coupled with HDH system	0.28	Giwa *et al.* (2016)
PVT-water coupled with HDH system	0.2	Gabrielli *et al.* (2019)
PVT-air coupled with HDH system	0.32	Present study

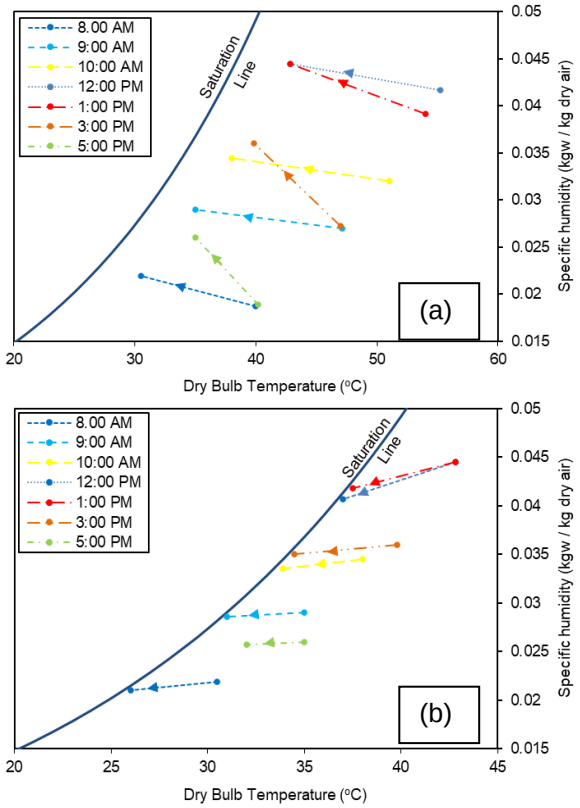

Fig 5. Psychometric properties of the air inside (a) the humidifier and (b) the dehumidifier of the PVT-HDH system.

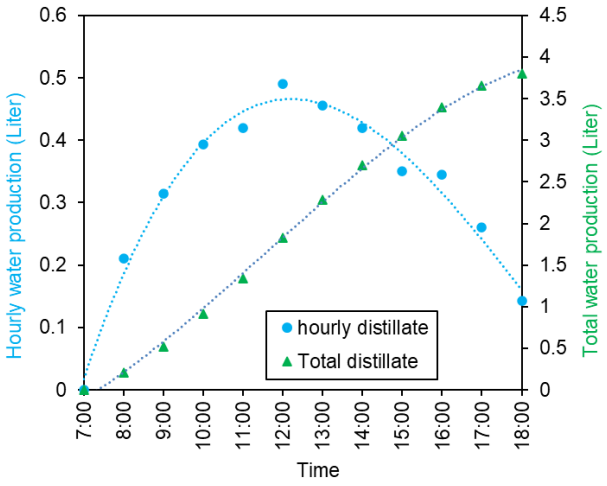

Fig 6. Water distillate production of the PVT-HDH system.

whereas air cooling is represented by a reduction in the dry bulb temperature. It is evident that both the dry bulb temperature and specific humidity of the air increased steadily until midday and then decreased until sunset. Moreover, the psychometric properties of the air through the humidifier and the dehumidifier are consistent with the results of Ghazy & Alrowais (2022).

The hourly and total water distillate of the humidification-dehumidification cycle is illustrated in Fig 6. Following the pattern of solar energy input, the hourly water distillate increased form morning to midday and then declined thereafter. The total water distillate of the PVT-HDH system was about 3.8 liters for a PV module surface area of 1.48 m × 0.68 m. These outcomes are considerably greater that the outcomes of the numerical simulation developed by Giwa et al. (2016), however, this can be attributed to the higher solar intensity measured in this study as compared to the solar intensity range considered in the simulation of Giwa et al. (2016). The distillate productivity of the current PVT-HDH system are compared to the productivity of other PVT-HDH systems in Table 3.

3.2 Electrical Performance

Fig 7(a) holds a comparison between the hourly current-voltage curves of the PV module in the PVT-HDH system and a conventional PV module with identical characteristics. It is observed that, for both PV modules, the short-circuit current noticeably increased from morning to noon as the incident solar irradiation remarkably increased and then noticeably decreased thereafter. In contrast, the open-circuit voltage of both PV modules decreased slightly throughout the day. Nevertheless, the hourly short-circuit current and open-circuit voltage of the PV module in the PVT-HDH system were typically greater than those of the standard PV module. These outcomes are in agreement with the outcomes of Jazayeri et al. (2013) and Zainal *et al.* (2016).

Subsequently, Fig 7(b) compares the hourly voltage-power characteristics of the PVT-HDH with those of the conventional PV module. The output power of both modules increased with the increase in solar irradiation from sunrise to noon, and then decreased until sunset. In addition, the output power of the PVT-HDH system was generally greater than that of the conventional PV module. These results agree well with the results of Zainal *et al.* (2016) and Jazayeri *et al.* (2013).

The maximum power outputs of both the PV module in the PVT-HDH and the conventional PV module is illustrated in Fig 8(a). The maximum power outputs of both modules constantly increased from morning to noon, and then decreased until sunset. In addition, the maximum power output of the PVT-HDH was always greater than that of the conventional PV. For instance, the maximum output power of the PVT-HDH system at midday was about 10 kW (20%) greater than that of the conventional PV module. These results agree well with the results of Jazayeri *et al.* (2013).

The short circuit currents of the PVT-HDH system and the conventional PV are illustrated in Fig 8(b). During the day, except for early morning and late afternoon, the PVT-HDH short circuit current is greater than that of the conventional PV. In addition, the short circuit current of both modules increased as solar irradiance increased form morning to midday and decreased as solar irradiance decreased thereafter.

Fig 8(c) shows the open circuit voltage of the PVT-HDH system and the conventional PV. The open circuit voltage of both modules constantly decreased throughout the day. In addition, the open circuit voltage of the PVT-HDH was always

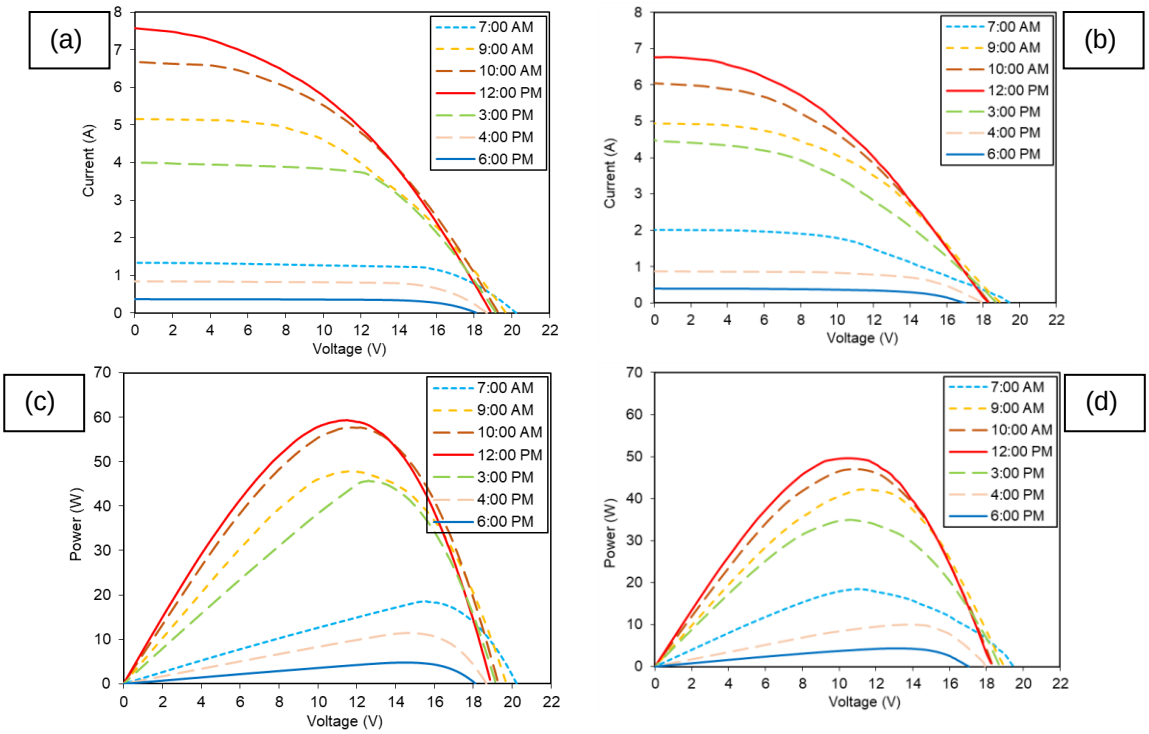

Fig 7. I-V curves for (a) the PVT-HDH system and (b) a conventional PV module, and P-V curves for (c) the PVT-HDH system and (d) a conventional PV module.

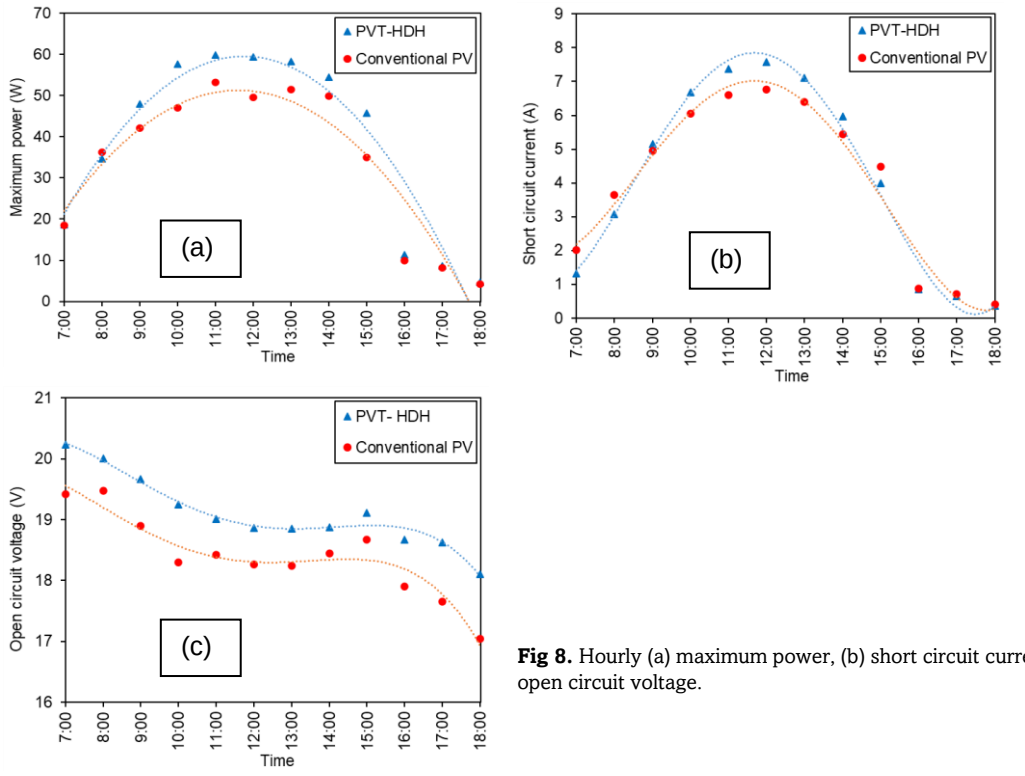

Fig 8. Hourly (a) maximum power, (b) short circuit current and (c) open circuit voltage.

greater than that of the conventional PV, with a range of 0.42 to 1 volt between the two open circuit voltages.

Finally, Fig 9 compares the electrical, thermal, and overall efficiencies of the PVT-HDH to the electrical efficiency of the conventional PV module. The efficiencies of the PVT-HDH system and conventional PV module decreased from morning to mid day due to the increase in thermal losses and the decrease in output electrical power with the increase in the temperature, and then remained constant for the rest of the day. In addition, the electrical efficiency of the PVT-HDH system was slightly greater than that of the conventional PV module. These results are in agreement with the measured data by Joshi *et al.* (2009). Moreover, the thermal efficiency of the PVT-HDH system was approximately 400% of its electrical efficiency, which significantly contributed to the overall efficiency of the PVT-HDH system in comparison to the conventional PV module.

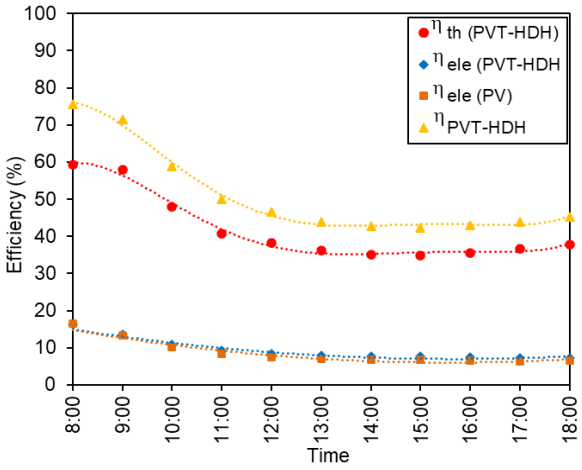

Fig 9. The efficiency of the PVT-HDH system as compared to conventional PV.

5. Conclusions

A hybrid PVT-air collector was constructed and combined with a closed air-heated HDH cycle. Air was circulated in the PVT collector to cool the PV module, then heated air was humidified by the spray of saline water, and finally, humid air was cooled and dehumidified inside a dehumidifier cooled by brine water to harvest potable water. To conserve condensation energy, the cooling water from the dehumidifier was used to humidify the air in the humidifier. The thermal and electrical performances of the PVT-HDH system were evaluated under the climate conditions of Sakaka (29.9° N, 39.3° E), Saudi Arabia, and compared to that of an identical PV module. The results showed a remarkable decrease in the temperature of the PV module in the PVT-HDH system as compared to that of the conventional PV module. This led to an increase of about 20% in the maximum output power of the PVT-HDH compared to the conventional PV module. In addition, the daily water distillate of the PVT-HDH system was about 3.8 liter for a PV module surface area of 1.48 m × 0.68 m resulting in a thermal efficiency of about 38% for the PVT-HDH system.

Acknowledgment

The author extends his appreciation to the Deputyship for Research & Innovation, Ministry of Education in Saudi Arabia for funding this work through project number "375213500". The author extends would like to extend his sincere appreciation to the central laboratory at Jouf University for supporting this study.

References

Abdul-Ganiy, S., Quansah, D. A., Ramde, E. W., Seidu, R. & Adaramola, M. S. (2021). Study effect of flow rate on flat-plate water-based photovoltaic-thermal (PVT) system performance by analytical technique. *Journal of Cleaner Production*, 321, 128985. https://doi.org/10.1016/j.jclepro.2021.128985

Alami, A.H. (2014). Effects of evaporative cooling on efficiency of photovoltaic modules. *Energy Convers. Manage.*, 77, 668-679. https://doi.org/10.1016/j.enconman.2013.10.019

Anand, B. & Srinivas, T. (2017). Performance Evaluation of Photovoltaic/Thermal–HDH Desalination System. *Applied Solar Energy,* 53(3), 243-249. https://doi.org/10.3103/S0003701X17030045

Antar, M. A. & Sharqawy, M. H. (2013) Experimental investigations on the performance of an air heated humidification-dehumidification desalination system, *Desalination Water Treat.*, 51, 837-843. http://dx.doi.org/10.1080/19443994.2012.714598

Bacha, H. B. (2013). Dynamic modeling and experimental validation of a water desalination prototype by solar energy using humidification dehumidification process. *Desalination,* 322, 182-208. http://dx.doi.org/10.1016/j.desal.2013.05.011

Bayrak, F., Oztop, H.F. & Selimefendigil, F. (2019). Effects of different fin parameters on temperature and efficiency for cooling of photovoltaic panels under natural convection. *Sol. Energy*, 188, 484-494. https://doi.org/10.1016/j.solener.2019.06.036

Brahim, T. & Jemni, A. (2017). Economical assessment and applications of photovoltaic/thermal hybrid solar technology: A review. *Sol. Energy,* 153, 540-561. https://doi.org/10.1016/j.solener.2017.05.081

Browne, M.C., Norton, B. & McCormack, S.J. (2016). Heat retention of a photovoltaic/thermal collector with PCM. *Sol. Energy*, 133, 533-548. https://doi.org/10.1016/j.solener.2016.04.024

Calise, F., Cappiello, F.L., Vanoli, R. & Vicidomini, M. (2019). Economic assessment of renewable energy systems integrating photovoltaic panels, seawater desalination and water storage. *Appl. Energy*, 253, 113575. https://doi.org/10.1016/j.apenergy.2019.113575

Deniz, E. & Cinar, S. (2016) Energy, exergy, economic and environmental (4e) analysis of a solar desalination system with humidification-dehumidification. *Energy Convers. Manag.*, 126, 12-19, http://dx.doi.org/10.1016/j.enconman.2016.07.064

Elsafi, A. M. (2017). Integration of humidification-dehumidification desalination and concentrated photovoltaic-thermal collectors: energy and exergy-costing analysis. *Desalination*, 424, 17-26. https://doi.org/10.1016/j.desal.2017.09.022

Fath, H. E. & Ghazy, A. (2002). Solar Desalination Using Humidification-Dehumidification Technology. *Desalination,* 142, 119-133. https://doi.org/10.1016/S0011-9164(01)00431-3

Fterich, M., Chouikhi, H., Bentaher & H., Maalej, A. (2018). Experimental parametric study of a mixed-mode forced convection solar dryer equipped with a PV/T air collector. *Sol. Energy,* 171, 751-760. https://doi.org/10.1016/j.solener.2018.06.051

Gabrielli, P., Gazzani, M., Novati, N., Sutter, L., Simonetti, R., Molinaroli, L., Manzolini, G. & Mazzotti, M. (2019). Combined water desalination and electricity generation through a humidification-dehumidification process integrated with photovoltaic-thermal modules: design, performance analysis and techno-economic assessment. *Energy Convers. Manage.*: X 1, 100004. https://doi.org/10.1016/j.ecmx.2019.100004

Ghazy, A. & Alrowais, R. (2022) Experimental Performance of Single-Slope Basin Solar Still Coupled with a Humidification–Dehumidification Cycle. *Sustainability*, 14, 15755. https://doi.org/10.3390/ su142315755

Ghazy, A. & Fath, H. E. (2016). Solar Desalination System of Combined Solar Still and Humidification-Dehumidification Unit. *Heat and Mass Transfer,* 52(11), 2497-2506. https://doi.org/10.1007/s00231-016-1761-1

Giwa, A., Fath, H. & Hasan, S. W. (2016). Humidification–dehumidification desalination process driven by photovoltaic thermal energy recovery (PV-HDH) for small-scale sustainable water and power production. *Desalination*, 377, 163-171. https://doi.org/10.1016/j.desal.2015.09.018

Hamed, M. H., Kabeel, A., Omara, Z. & Sharshir, S. (2015) Mathematical and experimental investigation of a solar humidification-dehumidification desalination unit. *Desalination,* 358, 9-17. http://dx.doi.org/10.1016/j.desal.2014.12.005

He, W., Xu, L. & Han, D. (2016b). Parametric analysis of an air-heated humidification-dehumidification (HDH) desalination system with waste heat recovery. *Desalination*, 398, 30-38. http://dx.doi.org/10.1016/j.desal.2016.07.016

He, W., Xu, L., Han, D. & Gao, L. (2016a). Performance analysis of an air-heated humidification-dehumidification desalination plant powered by low grade waste heat. *Energy Convers. Manag.*, 118, 12-20. http://dx.doi.org/10.1016/j.enconman.2016.03.073

Herrando, M., Pantaleo, A.M., Wang, K. & Markides, C.N. (2019). Solar combined cooling, heating and power systems based on hybrid PVT, PV or solar-thermal collectors for building applications. *Renew. Energy*, 143, 637-647. https://doi.org/10.1016/j.renene.2019.05.004

Jaszczur, M., Teneta, J., Hassan, Q., Majewska, E. & Hanus, R. (2021). An Experimental and Numerical Investigation of Photovoltaic Module Temperature Under Varying Environmental Conditions. *Heat Transfer engineering*, 42(3-4), 354-367. https://doi.org/10.1080/01457632.2019.1699306

Jazayeri, M., Uysal, S. & Jazayeri, K. (2013). A Simple Matlab/SIMULINK Simulation for PV Modules Based on One-Diode Model. *2013 High Capacity Optical Networks and Emerging/Enabling Technologies*, Magosa, Cyprus, 44-50. https://doi.org/10.1109/HONET.2013.6729755

Joshi, A. S., Tiwari, A., Tiwari, G. N., Dincer, I. & Reddy, B. V. (2009). Performance evaluation of a hybrid photovoltaic thermal (PV/T) (glass-to-glass) system. *Int. J. Thermal Sciences*, 48, 154-164. https://doi.org/10.1016/j.ijthermalsci.2008.05.001

Li, X., Yuan, G., Wang, Z., Li, H. & Xu, Z. (2014) Experimental study on a humidification and dehumidification desalination system of solar air heater with evacuated tubes. *Desalination*, 351, 1-8. http://dx.doi.org/10.1016/j.desal.2014.07.008

Mehrotra, S., Rawat, P., Debbarma, M., Sudhakar, K., Centre, E. & Pradesh, M. (2014). Performance of a solar panel with water immersion. *Int. J. Sci. Technol.*, 3, 1161-1172. https://www.ijset.net/journal/350.pdf

Monjezi, A. A., Chen, Y., Vepa, R., Kashyout, A. B., Hassan, G., Fath, H. E., Kassem, A. & Shaheed, M. H. (2020). Development of an off-grid solar energy powered reverse osmosis desalination system for continuous production of freshwater with integrated photovoltaic thermal (PVT) cooling. *Desalination*, 495, 114679. https://doi.org/10.1016/j.desal.2020.114679

Moss, R.W., Henshall, P., Arya, F., Shire, G.S.F., Hyde, T. & Eames, P.C. (2018). Performance and operational effectiveness of evacuated flat plate solar collectors compared with conventional thermal, PVT and PV panels. *Appl. Energy*, 216, 588-601. https://doi.org/10.1016/j.apenergy.2018.01.001

Narayan, G. P., Sharqawy, M. H., Lienhard V, J. H. & Zubair, S. M. (2010). Thermodynamic analysis of humidification dehumidification desalination cycles. *Desalination Water Treat.*, 16, 339-353. http://dx.doi.org/10.5004/dwt.2010.1078

Naroei, M., Sarhaddi, F. & Sobhnamayan, F. (2018). Efficiency of a photovoltaic thermal stepped solar still: Experimental and numerical analysis. *Desalination*, 441, 87-95. https://doi.org/10.1016/j.desal.2018.04.014

Nizetic, S., Coko, D., Yadav, A. & Grubisic-Cabo, F. (2016). Water spray cooling technique applied on a photovoltaic panel: The performance response. *Energy Convers. Manage.*, 108, 287-296. https://doi.org/10.1016/j.enconman.2015.10.079

Pham, T.T., Vu, N.H. & Shin, S. (2018). Design of curved fresnel lens with high performance creating competitive price concentrator photovoltaic. *Energy Procedia*, 144, 16-32. https://doi.org/10.1016/j.egypro.2018.06.004

Pourafshar, S. T., Jafarinaemi, K. & Mortezapour, H. (2020). Development of a photovoltaic-thermal solar humidifier for the humidification-dehumidification desalination system coupled with heat pump. *Solar Energy*, 205, 51-61. https://doi.org/10.1016/j.solener.2020.05.045

Rezvanpour, M., Borooghani, D., Torabi, F. & Pazoki, M. (2020). Using CaCl2·6H2O as a phase change material for thermo-regulation and enhancing photovoltaic panels' conversion efficiency: Experimental study and TRNSYS validation. *Renew. Energy*, 146, 1907-1921. https://doi.org/10.1016/j.renene.2019.07.075

Singh, D.B. (2018). Improving the performance of single slope solar still by including N identical PVT collectors. *Applied Thermal Engineering*, 131, 167-179. https://doi.org/10.1016/j.applthermaleng.2017.11.146

Singh, N.P. & Reddy, K.S. (2020). Inverse heat transfer technique for estimation of focal flux distribution for a concentrating photovoltaic (CPV) square solar parabola dish collector. *Renew. Energy*, 145, 2783-2795. https://doi.org/10.1016/j.renene.2019.07.122

Soufari, S., Zamen, M. & Amidpour, M. (2009a) Performance optimization of the humidification-dehumidification desalination process using mathematical programming. *Desalination*, 237, 305-317. http://dx.doi.org/10.1016/j.desal.2008.01.024

Soufari, S., Zamen, M. & Amidpour, M. (2009b) Experimental validation of an optimized solar humidification-dehumidification desalination unit. *Desalination Water Treat.*, 6, 244-251. http://dx.doi.org/10.5004/dwt.2009.494

Tiwari, G.N., Mishra, A.K., Meraj, Md., Ahmad, A. & Khan, M.E. (2020). Effect of shape of condensing cover on energy and exergy analysis of a PVT-CPC active solar distillation system. *Solar Energy*, 205, 113-125. https://doi.org/10.1016/j.solener.2020.04.084

Wang, J.-h., Gao, N.-y., Deng, Y. & Li, Y. l. (2012) Solar power-driven humidification-dehumidification (HDH) process for desalination of brackish water. *Desalination*, 305, 17-23. http://dx.doi.org/10.1016/j.desal.2012.08.008

Widyolar, B.K., Abdelhamid, M., Jiang, L., Winston, R., Yablonovitch, E., Scranton, G., Cygan, D., Abbasi, H. & Kozlov, A. (2017). Design, simulation and experimental characterization of a novel parabolic trough hybrid solar photovoltaic/thermal (PV/T) collector. *Renew. Energy*, 101, 1379-1389. https://doi.org/10.1016/j.renene.2016.10.014

Yildirim, C. & Solmus, I. (2014) A parametric study on a humidification-dehumidification (HDH) desalination unit powered by solar air and water heaters. *Energy Convers. Manag.*, 86, 568-575. http://dx.doi.org/10.1016/j.enconman.2014.06.016

Zainal, N. A., Ajisman & Yusoff, A. R. (2016). Modelling of Photovoltaic Module Using Matlab Simulink. *IOP Conf. Series: Materials Science and Engineering* 114, 012137. https://doi.org/10.1088/1757-899X/114/1/012137

Zamen, M., Amidpour, M. & Soufari, S. (2009) Cost optimization of a solar humidification dehumidification desalination unit using mathematical programming. *Desalination*, 239, 92-99. http://dx.doi.org/10.1016/j.desal.2008.03.009

Zhani, K., Bacha, H. B. & Damak, T. (2011) Modeling and experimental validation of a humidification-dehumidification desalination unit solar part. *Energy*, 36 (5), 3159-3169. http://dx.doi.org/10.1016/j.energy.2011.03.005